Chapter 4

Results & Discussion:

(Physical and thermal characterization of natural fibers)

Physical and thermal characterization of natural fibers

This chapter deals with the results and discussion of various physical characterization (SEM, FTIR, XRD) and thermal characterization (TGA/DSC) techniques employed for the evaluation of surface roughness, chemical modification (functional groups), crystallinity and thermal properties of the natural fibers under investigation.

4.1 Scanning electron microscopy (SEM)

4.1.1 SEM analysis of hemp fibers

Fig. 4.1 shows the SEM images of (A) untreated, (B) sodium carbonate treated, and (C) peroxide treated hemp fiber. From the Fig. 4.1, it can be observed that the surface morphology of hemp fiber changed considerably after both sodium carbonate and peroxide treatment. Fig. 4.1(A) shows that the untreated (UT) hemp fibers have waxes, lignin, and other surface impurities, while Fig. 4.1(B,C) shows that the sodium carbonate and peroxide treated fibers lack at least the majority of these surface impurities [75,76]. The presence of the surface impurities may have resulted in poor fiber–matrix interaction for UT hemp fiber reinforced eppxy composites (HFREC). This cleaning of the fiber surface by chemical modification has made the fiber surface rough and also has spitted the hemp fiber into finer fibers. This may be the reason for better fiber–matrix interlocking in treated HFREC [77].

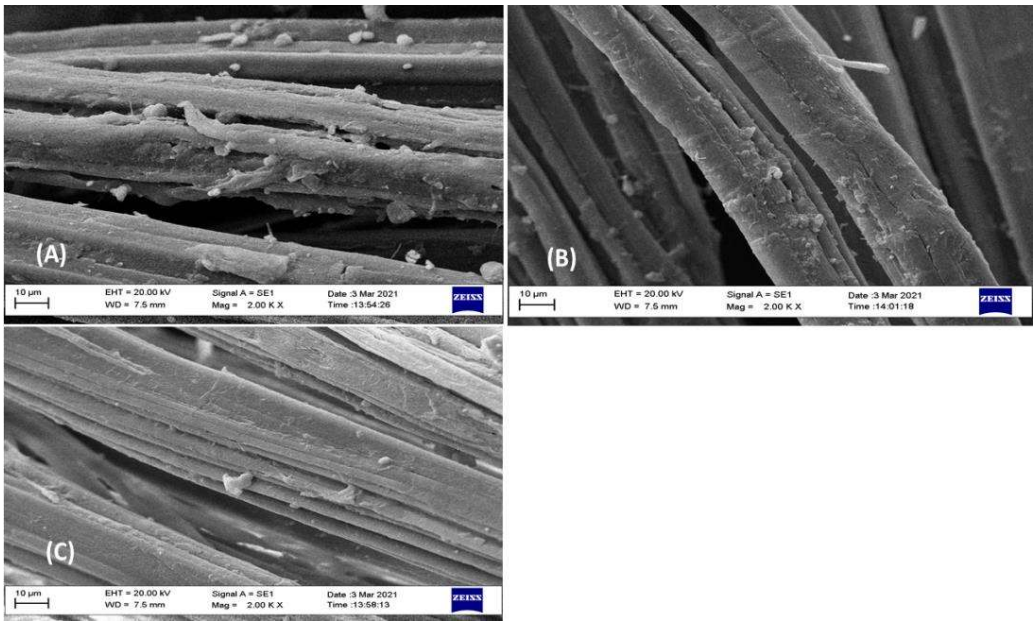

Figure 4.1 Scanning electron microscopy images of (A) untreated, (B) sodium carbonate treated, and (C) peroxide treated hemp fiber

Adhesion of fibers with polymers can be predicted by the SEM analysis of the fibers. Fig. 4.2 shows the SEM images of uncoated, PHB coated, and PLA coated hemp fibers. The surface of uncoated or raw hemp fiber was marked by the presence of several impurities like waxy amorphous substances as revealed in Fig. 4.2(A) [75,76]. These unwanted substances sticking to the fiber surface were responsible for poor fiber-matrix adhesion [62]. However, the SEM images from Fig. 4.1(B) and Fig. 4.1(C) of hemp fibers coated with PHB and PLA showed that the unwanted amorphous substances and other impurities were removed from the fiber surface and fibrillation was also observed for the coated fibers. This may be because of the sodium hydrogen carbonate treatment of the fibers prior to the polymer coating. Furthermore, both PHB and PLA are both poth polymers and polymers are usually hydrophobic in nature, as a result of this, PHB and PLA coating over the natural fibers has the ability to transform the hydrophilic nature of natural fibers into hydrophobic nature, which may improve the fiber-matrix adhesion [44-46].

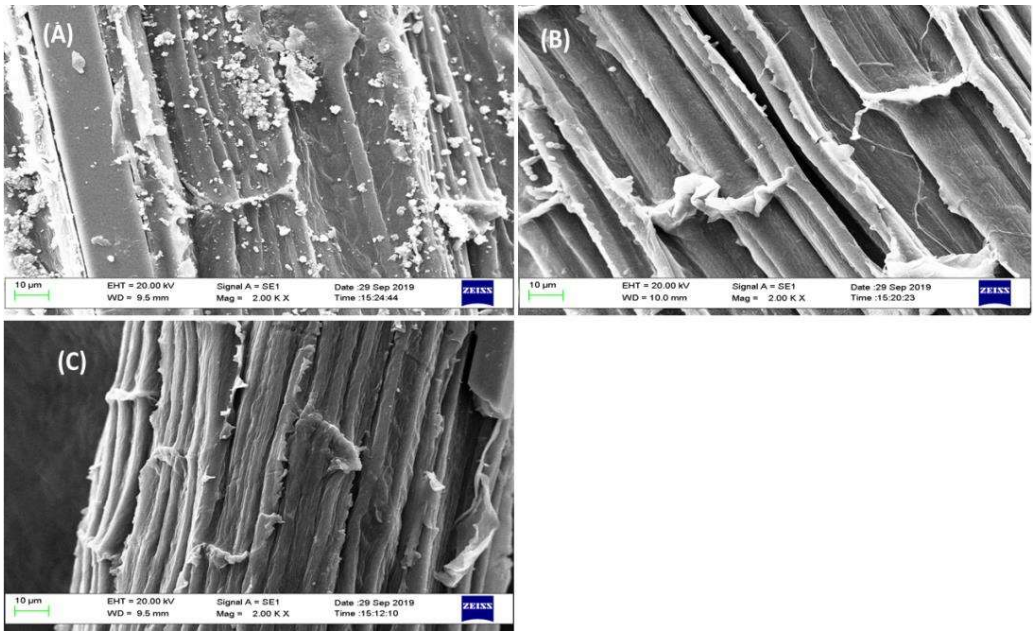

Figure 4.2 SEM images of (A) untreated hemp fiber, (B) PHB coated hemp fiber, and (C) PLA coated hemp fiber.

4.1.2 SEM analysis of sisal fibers

Fig. 4.3 shows the scanning electron micrographs (SEM) of the surfaces of untreated (UT), alkali (AT), glutamic acid (GT), and combination of alkali and glutamic acid (AGT) treated sisal fibers. The existence of wax, lignin, hemicellulose, silica, pectin, and other impurities can be seen on the surface of the UT fibers and were primarily accountable for the poor fiber-matrix adhesion as shown in Fig. 4.3(A). The existence of lignin and pectin makes the surface of UT fiber smooth [75,76]. Alkali treatment was accountable for the eviction of lignin and other contaminants from the surface of the fiber. Because of this, the surface roughness of the fiber got increased and the diameter of the fiber got reduced as observed in Fig. 4.3(B). This may be the reason for the improvement in fiber-matrix bonding. The existence of a covering on the GT and AGT fiber surface can be seen in Fig. 4.3(C,D). From this, it can be concluded that the glutamic acid got deposited on the fiber surface.

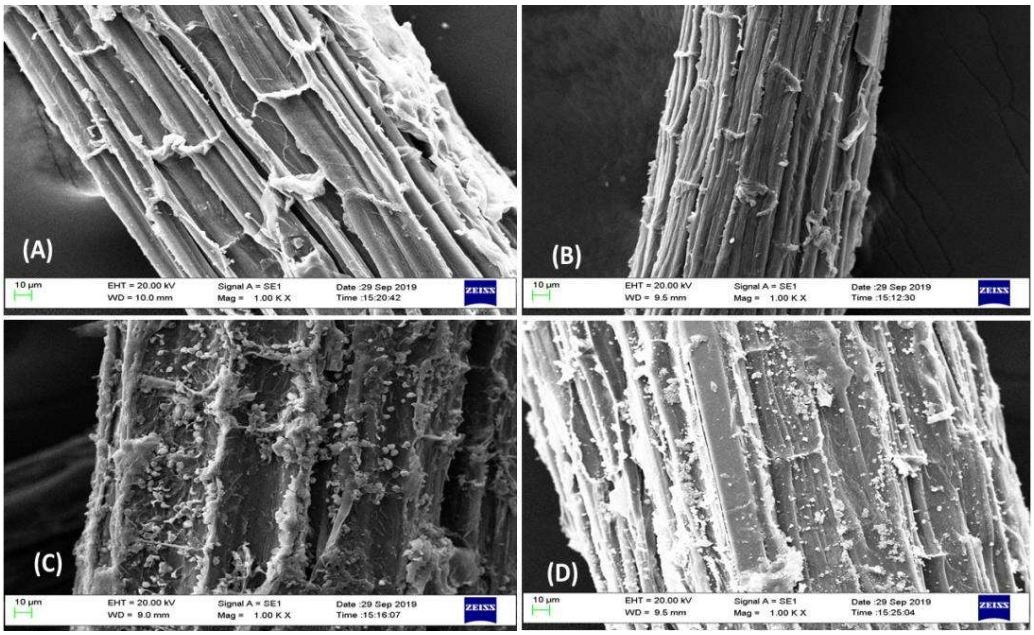

Figure 4.3 SEM micrographs of (A) UT (B) AT (C) GT and (D) AGT sisal fibers.

The changes in the surface morphology of the untreated and treated sisal fibers were investigated by scanning electron microscopy (SEM) as shown in Fig. 4.4. Waxes, lignin, and other components are present on the surface of untreated fibers, whereas stearic acid and sodium citrate treated fibers lack at least some of these compounds. The hydrophilic character of fiber is due to these non-cellulosic components, which results in poor interfacial bonding with the hydrophobic polymer matrix [75]. The sodium citrate treatment employed in this investigation was the most effective approach for removing the chemicals from the sisal fiber surface, as shown by the micrographs in Fig. 4.4(C). These treatments depolymerize cellulose, expose the short length cellulose fibril, and remove a certain percentage of lignin, wax, and hemicelluloses from the fiber cell wall [78]. This could have improved the surface roughness of the treated fibers which may be responsible for enhanced fiber-matrix adhesion.

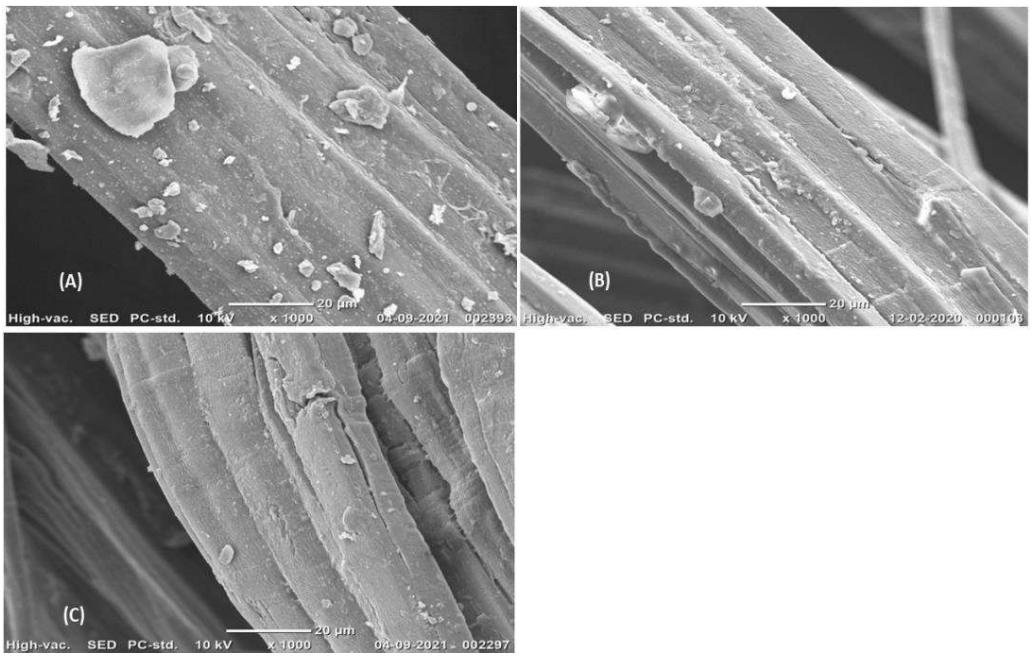

Figure 4.4 SEM images of (A) untreated, (B) stearic acid treated, and (C) sodium citrate treated sisal fiber

4.1.3 SEM analysis of jute fibers

Figure 1 shows the morphological or structural changes in the jute fiber both before and after chemical modification. The SEM micrograph of untreated jute fibre (Fig. 4.5(A)) revealed the existence of several impurities, cellulosic compounds, and amorphous waxy cuticle coating on the fiber and the structure of the untreated fiber appears to be closely packed [75,76]. The creation of a fragile fiber-matrix bond is induced by these impurities. However, all the fibers treated with chemicals (Fig. 4.5(B,C and D)) revealed that the waxy coating and impurities had been stripped from the surface and that the treated surface of the fiber had been much rougher. From the Fig. 4.5(B,C and D), it can be seen that the surface modification has broken the fiber into finer fibers. This may contribute to high fibre and matrix interlocking and adhesion [78].

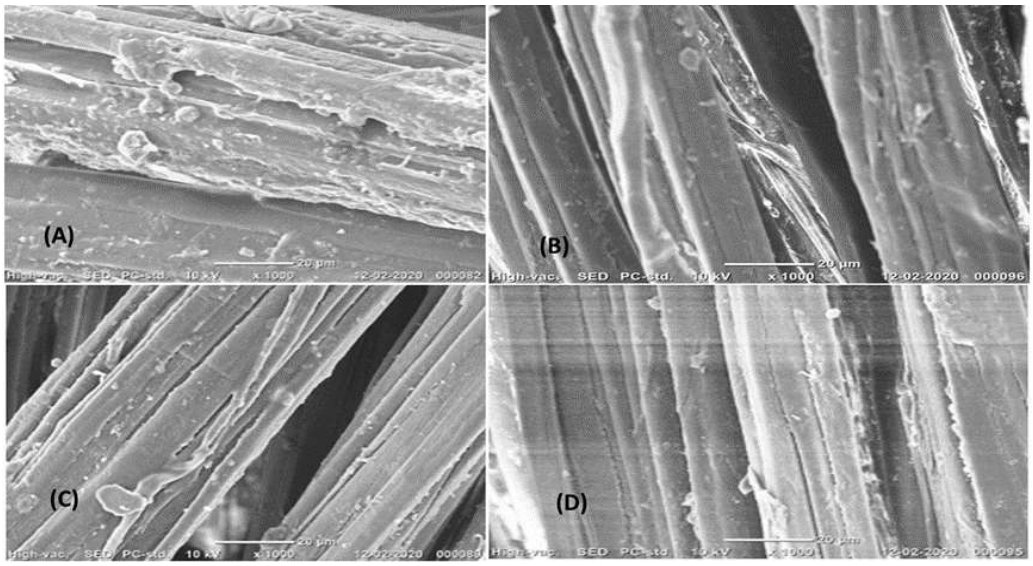

Figure 4.5 SEM images of (A) UT (B)AT (C) ST and (D) SHT jute fiber.

4.2 Fourier transform infrared spectroscopy (FTIR)

4.2.1 FTIR analysis of hemp fibers

FTIR spectra of UT, ST, and PT hemp fibers are shown in Fig. 4.6, and the FTIR peaks and their possible assignments were provided in Table 4.1. The peak at 2921 cm^{-1} for UT hemp fiber represents the aliphatic CH_2- stretching vibration of functional groups of alkanes (cellulose and lignin) and carboxylic acid; however, this peak is shifted to 2920 and 2916 cm^{-1} for PT and ST fibers [79]. The peak at 2360 cm^{-1} for UT hemp fibers represents the C═C stretching vibration for impurities like wax present on the fiber surface; however, this peak is absent in ST hemp fiber and shifted to 2320 cm^{-1} for PT hemp fiber confirming that the sodium carbonate and peroxide treatment was responsible for complete and partial elimination of wax from the fiber surface, respectively [80]. The peak at 1731 cm^{-1} for UT hemp fiber represents the C═O stretching of carbonyl groups in hemicellulose; however, this peak is absent in both ST and PT hemp fiber, which suggests that both the chemical treatments were

successful in removing hemicellulose from the surface of the fiber [81]. The peak at 1643 cm^{-1} for UT fiber represents the C═C stretching bond structure from the functional groups of alkene presents in lignin, but this peak is shifted to 1592 and 1590 cm^{-1} for ST and PT fiber, respectively, confirming that the lignin content of the fiber was partially removed by both sodium carbonate and peroxide treatment [82]. The peak that occurred at 1240 cm^{-1} for the UT fiber indicates the C- O- C stretching of the functional group found in hemicellulose [83]. The peak appeared at 1156 cm^{-1} for UT fiber is due to the absorption peak of cellulose; however, it is shifted to 1160 and 1158 cm^{-1} for ST and PT fiber, respectively [84]. The peak that occurred at 1029 cm^{-1} is due to the C-O and O-H stretching vibrations of polysaccharides found in cellulose. The peak that appeared at 667 cm^{-1} is due to the C-OH out-of-plane bending [85].

Table 4.1. FTIR peak analysis of untreated and treated hemp fiber.

Wave number (cm^{-1})			Possible assignments
UT Fiber	ST fiber	PT fiber	
2921	2916	2920	Aliphatic CH_2 stretching (cellulose and lignin)
2360	-	2320	C=C stretching (impurities like wax)
1731	-	-	C=O stretching (hemicellulose)
1643	1592	1590	C=C stretching (lignin)
1240	1236	1235	C-O-C stretching
1029	1030	1032	C-O and O-H stretching (cellulose)
667	661	660	C-OH out of plane bending

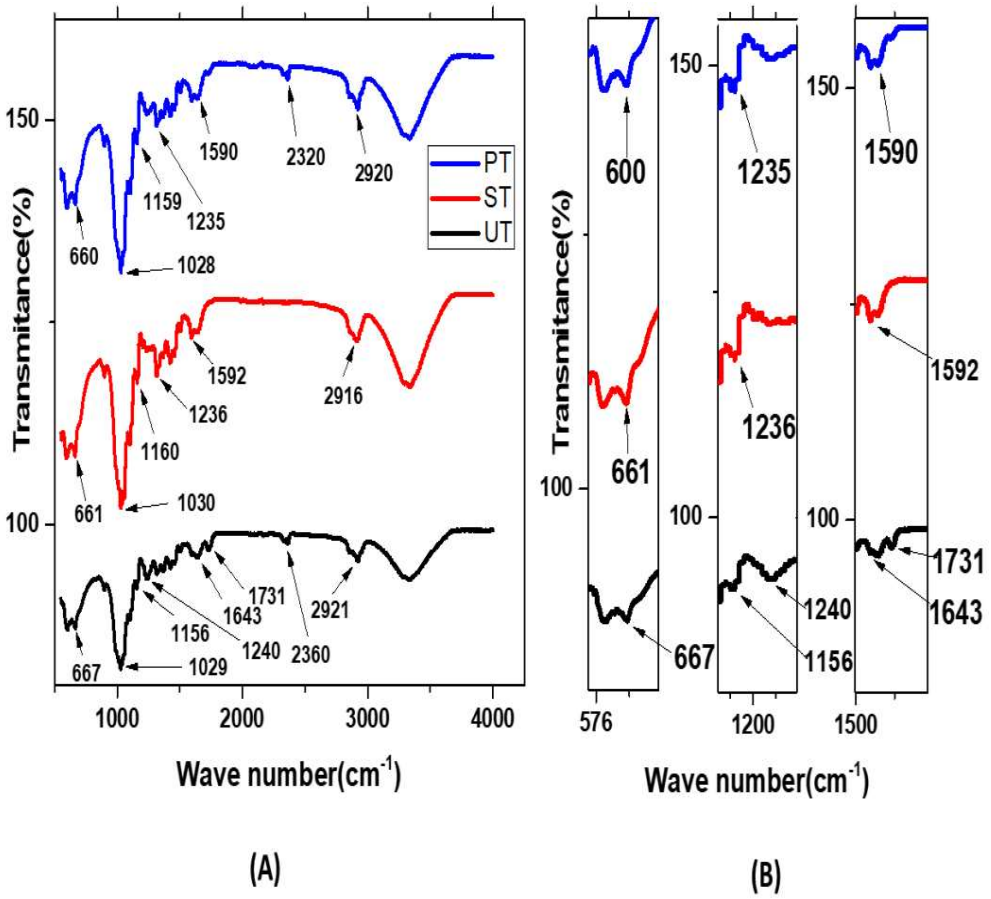

Figure 4.6 (A) Comparative Fourier transform infrared (FTIR) spectra of untreated (UT), sodium carbonate treated (ST), and peroxide treated (PT) hemp fibers. (B) Zoom in of FTIR spectra.

4.2.2 FTIR analysis of sisal fibers

The infrared detection and the analysis of fibers treated by various chemical treatment methods were done to examine the changes that occur in the chemical bonds and structure of fibers [84]. A comparative FTIR analysis of both raw and modified sisal fibers was made and displayed in Fig. 4.7. The FTIR spectrum of UT sisal fibers emphasizes on the most interesting transmittance peaks. The peak identified at 3326 cm^{-1} represents the hydrogen bonded OH stretching vibrations [85]. The peak at 2916 cm^{-1} corresponds to the C-H stretching in cellulose [83]. The band at 1734 cm^{-1} and 1600 cm^{-1} can be attributed to the carbonyl group and aromatic ring stretching (C = C)

respectively [82]. Another peak at 1418 cm^{-1} can be caused by the bending of symmetric CH_2 in cellulose [81]. The transmittance at 1316 cm^{-1} is owing to the bending of C-O groups of the aromatic ring [80]. The peak at 1028 cm^{-1} is generated by stretching of C-O-C [79]. The small band at 896 cm^{-1} can be readily assigned to the beta-glycosidic linkages between the monosaccharides [85]. The effects of chemical treatment on sisal fibers were also determined using FTIR. Here in the UT sisal fiber, the peak at 1734 cm^{-1} corresponding to C = O stretching of carbonyl ester is not visible in the chemically modified fibers. A change can be seen when a peak at 2361 cm^{-1} which is attributed to the C-O stretching of acetyl group for UT untreated sisal fiber is shifted to 2359 cm^{-1} for alkali-treated sisal fiber [86]. In alkali-treated sisal fibers, peak at 1506 cm^{-1} represents C = C stretching of the aromatic ring but the other three, i.e., UT, GT, and AGT, fibers did not show any peak of transmittance. Also, only GT and UT sisal fibers show a peak of transmittance at 1242 cm^{-1} which is because of C-O stretching vibration of the acetyl group in lignin [77].

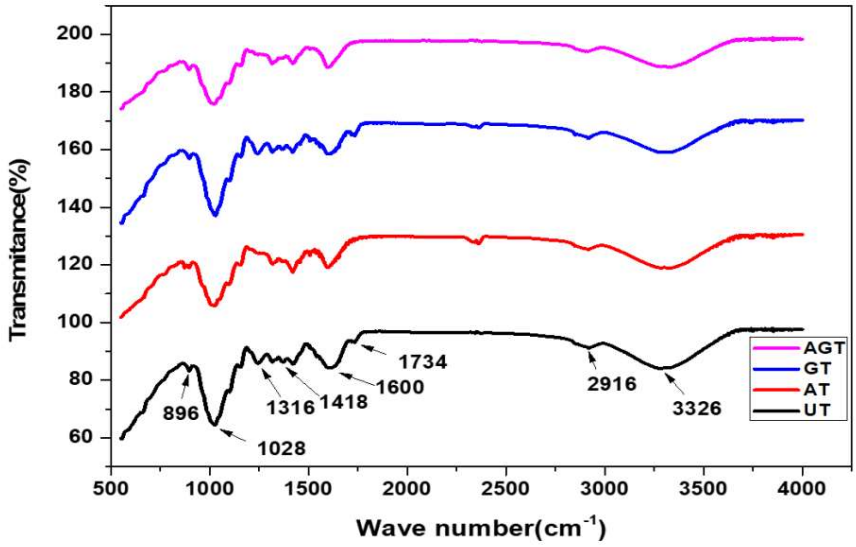

Figure 4.7 Comparative FTIR spectra of UT, AT, GT and AGT sisal fiber

FTIR analysis of the untreated and treated fibers were done to observe the changes in the chemical structure of the fibers as shown in Fig. 4.8. All of the spectra were baseline adjusted to the peak focused at 3337 cm^{-1}, which was assigned to the O-H stretching vibration and hydrogen bond of the hydroxyl group, as stated by literature [80]. The FTIR spectra of untreated and stearic acid treated fiber revealed a distinctive band at about 2923 cm^{-1} owing to C–H stretching vibrations of methylene groups, as illustrated in Fig. 4.8 [79]. The peak located at 1732 cm^{-1}, which is attributable to the C=O stretching vibration of carboxylic acid linkage in lignin or ester group in hemicellulose, seems to disappear in both sodium citrate and stearic acid treated fiber [81]. This finding suggested that the surface treatments were effective in removing waxy compounds from the untreated sisal fibers. The peak seen at 1643 cm^{-1} for untreated sisal fiber corresponds to the bending of the C=C bond structure observed in lignin, however this peak is absent from FTIR spectra of sodium citrate and stearic acid fibers, indicating that all chemical treatment procedures were effective in eliminating part of the lignin content from the fiber surface [82]. In the spectra of treated fibers, there is also a decrease of the peak located at 1240 cm^{-1}, which is caused by the C-O stretching vibration of the acetyl group in lignin [84]. No additional significant alterations can be seen in the FTIR spectra of the treated sisal fiber.

4.2.3 FTIR analysis of jute fiber

Alkali treated (AT), Na_2CO_3 treated (ST), $NaHCO_3$ treated (SHT) and untreated (UT) jute fibers were analyzed in FTIR, and FTIR spectra for the chemically modified fibers and untreated fibers were represented in Fig. 4.9. The peak identified at 3332 cm^{-1} represents the hydrogen bonded OH stretching vibrations [82]. The peaks

observed at 2920 cm^{-1} is due to the saturated C-H stretching vibration [86]. The peak appeared at 1731 cm^{-1} for UT jute fiber corresponds to the stretching of C=O of carbonyl groups found in hemicellulose, but this peak is not visible in AT, Na_2CO_3 treated and $NaHCO_3$ treated jute fiber confirming that the hemicellulose content was removed by the chemical treatments [84]. The peak observed at 1643 cm^{-1} for UT jute fiber corresponds to the stretching of C=C bond structure found in lignin, however this peak is not present in any of the chemically treated fiber which indicates that all the chemical treatment methods were successful in removing the lignin content from the fiber [83]. The peaks due to stretching of C-O and O-H found in cellulose is observed at 1029 cm^{-1}.

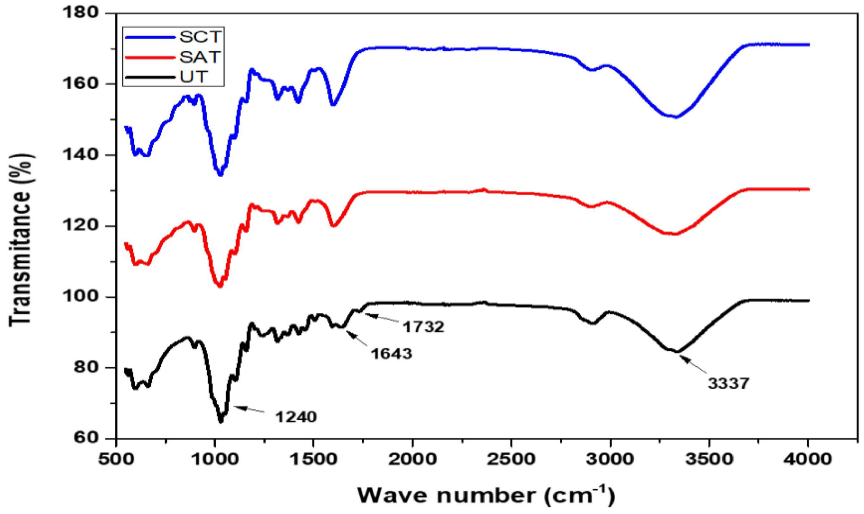

Figure 4.8 Comparative FTIR spectra of UT, SAT and SCT sisal fiber

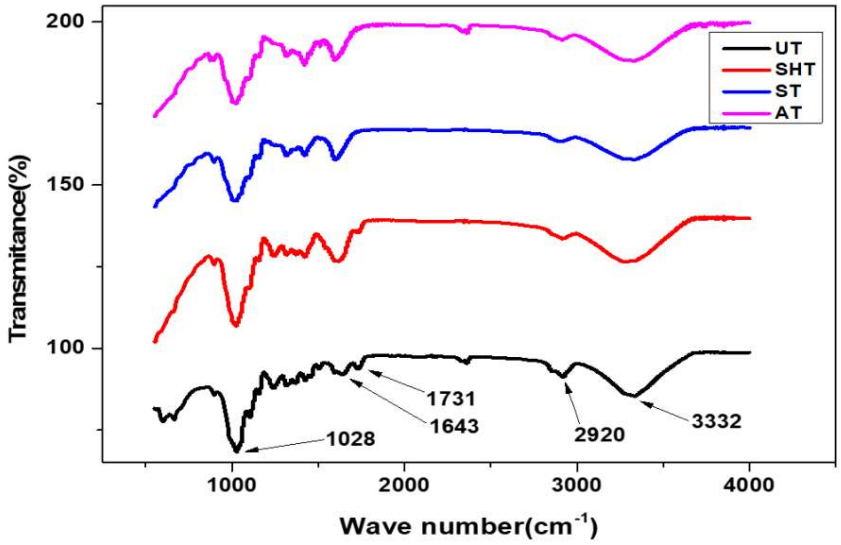

Figure 4.9 Comparative FTIR spectra of UT, AT, ST and SHT jute fiber

4.3 X-Ray diffraction (XRD)

4.3.1 XRD analysis of hemp fibers

The crystalline and structural properties of UT, ST, and PT hemp fibers were studied by using the XRD technique and their XRD patterns are shown in Fig. 4.10 [87]. The major crystalline peak (I_{002}) occurred within a range of 21.96°–22.97° of the 2θvalues for each profile and the amorphous peak (Iam) occurred within a range of 17.87°–19.06° of the 2θ values for each profile [88-89]. It is quite clear from Fig. 4.10 and Table 4.2 that the sodium carbonate and peroxide treatment of hemp fiber have increased the I_C of the fiber. There is an enhancement of 1.8% and 5.2% in I_C of ST and PT hemp fiber over UT fiber. The highest crystallinity index was obtained for the PT fiber followed by ST fiber. The high crystallinity index was due to the effective removal of impurities and hemicellulose, which was also seen in other cellulose fibers such as jute treated with alkali and alfa fiber treated with alkali [90-91]. Razak et al. [92] also reported a higher crystallinity index of the hemp fiber when they work with

PT fiber. Elimination of amorphous materials by chemical treatment results in improved packing and stress relief of cellulose, which may have contributed to the improvement in I_C of treated fibers [86,93].

XRD analysis of uncoated, PHB coated, and PLA coated hemp fibers were done to study their crystalline properties and their XRD patterns are represented in Fig. 4.11. Crystallinity index of the fibers are represented in Table 4.3. The highest diffraction intensity (I_{002}) of the crystalline substances of the fibers and the lowest diffraction intensity (Iam) of the amorphous substances of the fibers occurred within a range of 23.64° to 22.12° and 19.41° to 18.20°, respectively, at the 2θ values for each profile. From the Fig. 4.11 and Table 4.3, it is quite evident that the PHB coated and PLA coated hemp fibers had an improvement of 4.8% and 11.3% in crystallinity index when compared to the uncoated hemp fiber. This improvement in Ic may be due to the removal of amorphous constituents from the fiber surface done by the sodium hydrogen carbonate treatment of the fiber prior to the coating [89,90]. Also, the coating of polymer may have contributed to the improvement of crystallinity index because crystallization can also be induced by polymerization and this case, crystallization may have been triggered by molecule orientation in the stretch direction of the polymer coatings.

Table 4.2 Comparison of crystallinity index (I_C) of untreated and treated hemp fiber.

Fiber treatment	I_{am}	I_{002}	I_C
UT fiber	4084	12706	0.678
ST fiber	4393	14209	0.690
PT fiber	3238	11325	0.714

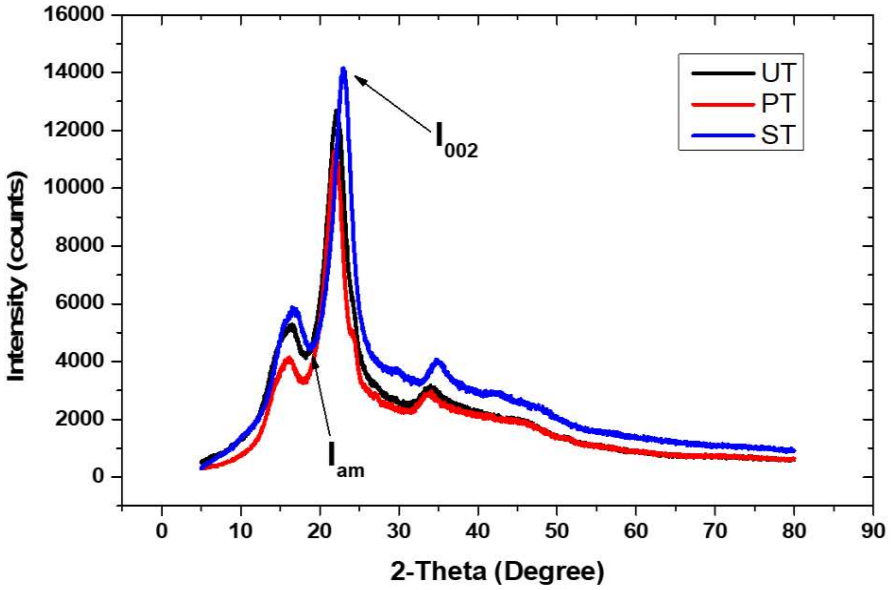

Figure 4.10 X-ray diffraction patterns of untreated (UT), sodium carbonate (ST), and peroxide treated (PT) hemp fibers.

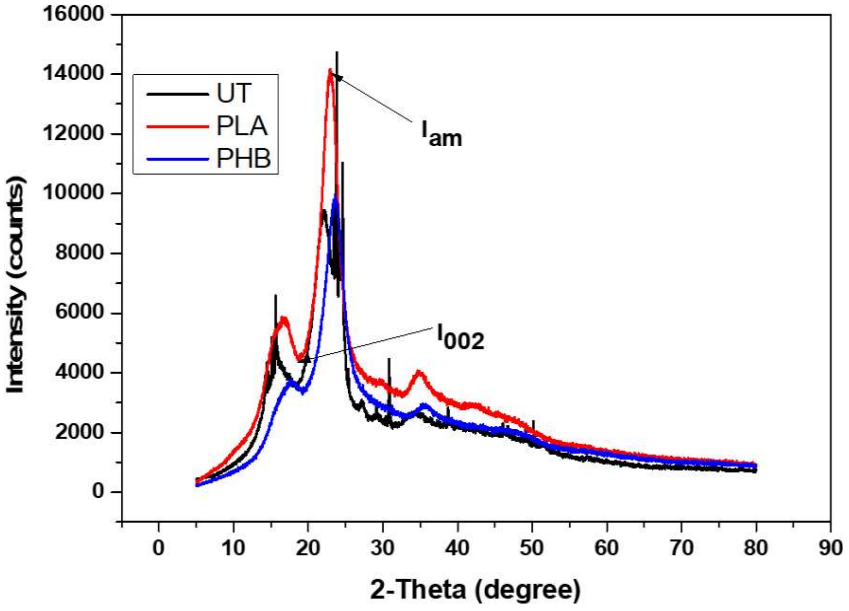

Figure 4.11 XRD patterns of untreated hemp fiber, PHB coated hemp fiber, and PLA coated hemp fibers.

Table 4.3 Comparison of crystallinity index (I_C) of untreated and coated hemp fiber.

Fiber treatment	Crystallinity index (I_C)
UT fiber	0.62
PHB coated fiber	0.65
PLA coated fiber	0.69

4.3.2 XRD analysis of sisal fibers

The cell wall of the plant fiber is composed of cellulose, hemicellulose, and lignin. Cellulose includes crystalline and amorphous regions, while hemicellulose and lignin have only amorphous region [86]. The XRD analysis gives information about the crystallinity and structural features of sisal fibers before and after chemical treatment [87]. X-Ray diffractograms of UT, AT, GT, and AGT sisal fibers were shown in Fig. 4.12. From Fig. 4.12, it can be observed that the crystalline peak (I_{002}) at 2θ value of each profile is ranging from 21.96^o to 22.37^o and the amorphous peak (Iam) at 2θ value is ranging from 17.28^o to 18.28^o. The X-Ray diffractograms show that there is an increase in the intensity of the crystallographic plane with chemical modification of fibers and AGT fibers show the maximum intensity. Table 3 shows the crystallinity index of raw and modified fibers. The crystallinity index of UT, AT, GT, and AGT fibers were found to be 0.50, 0.63, 0.53, and 0.64, respectively. Here, the crystallinity index of sisal fiber found to have increased with chemical treatments, and the highest crystallinity index was observed for the AGT fibers followed by GT and AT fibers [89]. Amorphous constituents like hemicellulose, pectin, lignin, etc. are removed which results in an increase of the crystallinity index of treated fibers [90,92].

Mohanta and Acharya [86] also reported similar observations when they worked with NaOH treatment of luffa cylindrica. The increase in crystallinity after the chemical treatment may have improved the adhesion between fiber and matrix [93].

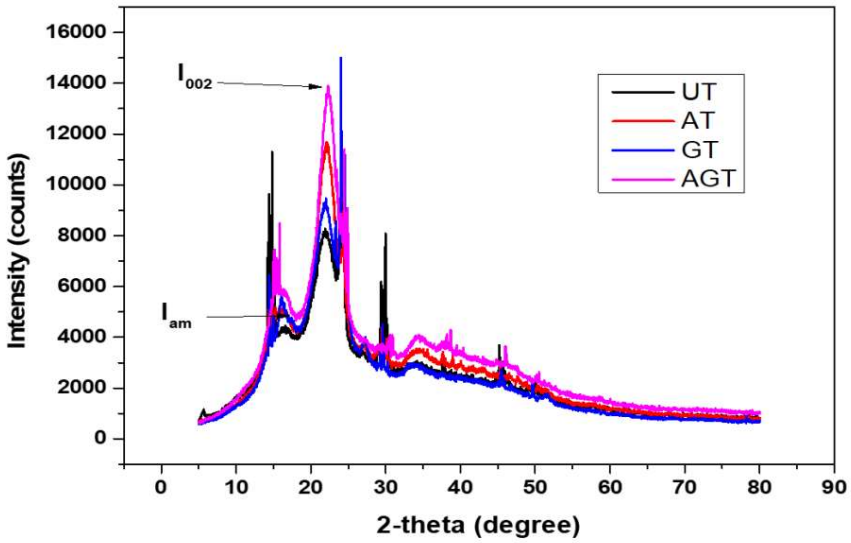

Figure 4.12 XRD patterns of UT, AT, GT and AGT sisal fibers

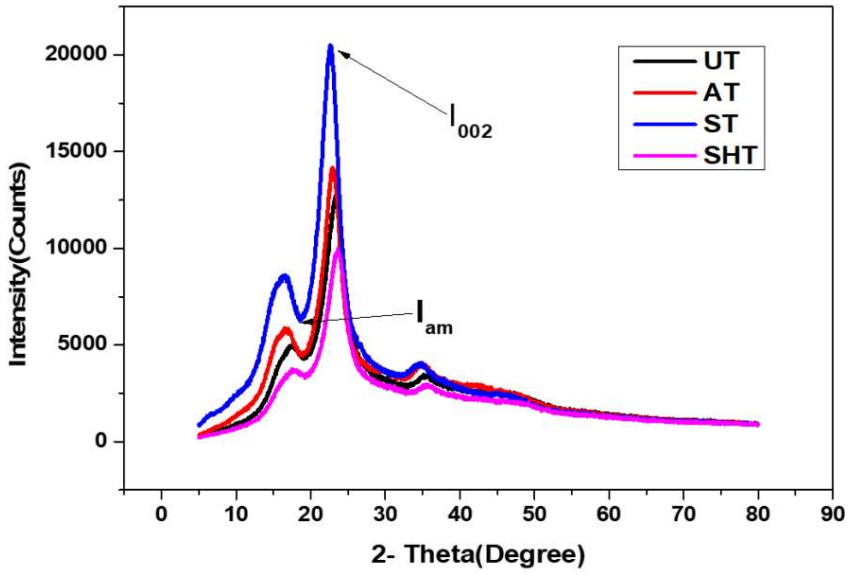

Figure 4.13 XRD patterns of UT, AT, ST and SHT jute fibers

4.3.3 XRD analysis of jute fibers

The XRD study showed the constructional and crystallinity behaviour of jute fiber before and after chemical modification with NaOH, Na_2CO_3 and $NaHCO_3$ [89]. X-Ray diffraction patterns of un-modified, NaOH, $NaHCO_3$, and Na_2CO_3 modified fibers were shown in Fig. 4.13. It is found that the main crystalline peak (I_{002}) in each profile happened at approximately 2θ values in the range from 22.63° to 23.64°, reflecting the crystallographic plane of cellulose (002). However, each profile's amorphous peak (I_{am}) was between 18.72° and 19.41° at the 2θ-value. From Fig. 4.13 and Table 4.4, it is evident that the chemical modification has improved the crystallinity index of the jute fiber. The highest I_C was observed for SCT fiber which is around 0.693 and the lowest I_C was observed for UT jute fiber which is around 0.667 [91]. NaOH treated, Na_2CO_3 treated, and $NaHCO_3$ treated fibers have an improvement of 3.3%, 3.9%, and 1.2% of I_C over untreated jute fiber. Increase in crystallinity of the modified fibers is due to elimination of pectin and amorphous materials from the fiber after chemical treatment [93].

Table 4.4 Comparison of crystallinity index (I_C) of untreated and treated jute fiber.

Fiber treatment	Maximum intensity (I_{am})	Maximum intensity (I_{002})	Crystallinity index (I_C)
UT fiber	4265	12816	0.667
AT fiber	4394	14166	0.689
ST fiber	6275	20471	0.693
SHT fiber	3239	9995	0.675

4.4 Thermal characterization of fibers

4.4.1 Thermogravimetric analysis (TGA) of sisal fibers

Fig. 4.14 shows TGA curves of raw and chemically treated sisal fibers. Thermal deterioration happened in three phases, as shown by the curves. The initial weight loss was roughly 4-7 percent and occurred at temperatures below 100°C. The first step of the thermal degradation process occurred between 50°C and 185°C and was caused by the removal of certain waxy elements and moisture contents from the fibers, with a weight loss of roughly 8-9% in this temperature range. The second deterioration stage occurred at a temperature range between 220°C and 370°C, potentially due to hemicellulose and alpha-cellulose degradation [94,95]. In this temperature range, UT and SAT treated fibers lost roughly 64% and 66% respectively of their weight, whereas SCT treated fibers lost around 68% of their weight. The last stage of deterioration occurred between 380°C and 590°C and corresponds to the breakdown of lignin and other non-cellulosic components found in the fibers [96]. In this temperature range, UT and SAT treated fibers lost roughly 12% and 13% respectively of their weight, whereas SCT treated fibers lost around 21% of their weight. This suggests that the thermal stability of the fibers was slightly reduced after the chemical treatment.

Table 4.5 Thermal properties of untreated and surface modified sisal fibers obtained from DSC curves.

Sample	Endothermic peak (°C)	First exothermic peak (°C)	Second exothermic peak (°C)
UT fiber	68.74	339.23	395.17
SAT fiber	61.13	328.12	392.32
SCT fiber	59.52	326.21	389.11

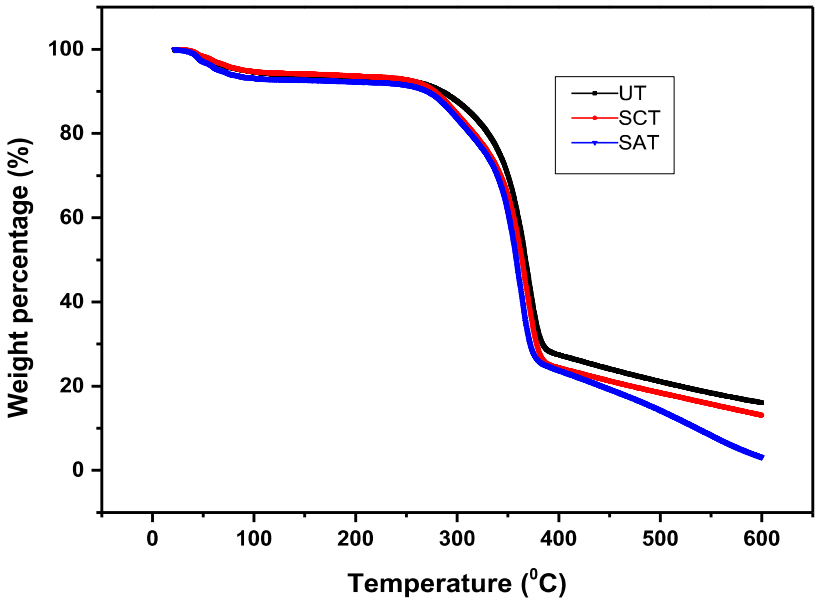

Figure 4.14 TGA curves of UT, SCT and SAT sisal fibers.

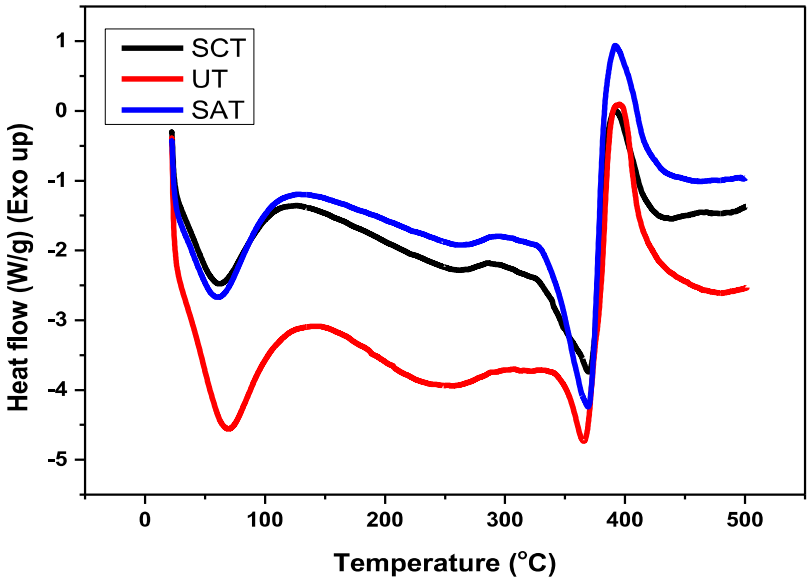

Figure 4.15 DSC curves of UT, SCT and SAT sisal fibers.

4.4.2 Differential scanning calorimetry (DSC) analysis of sisal fibers

The typical DSC curves for both untreated and surface modified sisal fibers are shown in Fig. 4.15 and Table 4.5 lists the critical exothermic and endothermic peak temperatures. The DSC profiles of the untreated and chemically treated fibers are fairly similar. One endothermic peak and two exothermic peaks make up the three main peaks for each fiber sample. Both the raw and chemically treated fibers exhibit a broad endothermic peak in the temperature range of 55°C-70°C, which is due to the vaporization of water absorbed in the fibers [97]. No exothermic or endothermic reaction peaks are visible within the temperature range 150°C-240°C, suggesting that the fibers were stable within that temperature. The first exothermic peak in the DSC curve for untreated fiber is visible at around 339.23°C, which is caused by thermal degradation of hemicellulose and glycosidic linkages of cellulose [98]. However, this peak gets shifted to 328.12°C and 326.21°C for SAT fibers and SCT fibers, respectively. The very prominent second endothermic peak for the untreated fiber was observed at about 395.17°C demonstrating the degradation of cellulose, resulting in the formation of char. However, for SAT fiber and SCT fiber, this second endothermic peak was observed at about 392.32°C and 389.11°C, respectively. This slight reduction in the decomposition temperature of the chemically treated fibers may have reduced the thermal stability of the treated fibers.

Chapter summary

The following topics are discussed in this chapter:

- The results and discussions of various physical characterization (SEM, FTIR, XRD) and thermal characterization (TGA/DSC) techniques employed for the evaluation of surface roughness, chemical modification (functional groups), crystallinity and thermal properties of the natural fibers under investigation.

The results and discussion of the water absorption, mechanical and tribological properties of the NFRECs will be presented in the next chapter.